Stirling machine for cooling production at intermediate temperature range

S. Djetel-Gothe[1], M.Z. Getie[1,2,3], F. Lanzetta[1], S. Bégot[1], E. Gavignet[1]

[1] FEMTO-ST Institute, Univ. Bourgogne Franche-Comté, CNRS, Belfort, France
[2] Bahir Dar Energy Center, Bahir Dar Institute of Technology, Bahir Dar University, Bahir Dar, Ethiopia
[3] Faculty of Mechanical and Industrial Engineering, Bahir Dar Institute of Technology, Bahir Dar University, Bahir Dar, Ethiopia

E-mail : francois.lanzetta@univ-fcomte.fr

Abstract. The Stirling technology presents an opportunity to achieve environmental protection in terms of greenhouse gas emissions and global warming. It is an alternative technology to vapour compression cycles that use refrigerant fluids. The described system is a Beta Stirling refrigerator working with nitrogen for cooling production at moderate temperature. The cooling performances are studied under different rotational speeds and heat loads. We have carried out experimental results with heat load to simulate the cooling capacity from 0 W (no load) to 650 W in the cooling temperature range -70°C to 20°C. The coefficient of performances and cooling efficiency are discussed.

1. Introduction

The climate impact of cooling equipment, including fridges, heat pumps and air-conditioners, has been increasing rapidly in recent decades. These systems use huge amounts of electricity and often rely on super-polluting refrigerant gases such as hydrofluorocarbons (HFCs) [1-3]. A Stirling refrigerator cycle works with a working gas like air, helium or hydrogen and these gases are environmental friendliness. Based on the idea of J. Herschel's in 1834 to use a Stirling engine in reverse and cooling mode, A. Kirk in 1874 built the first refrigerating machine [4]. The commercial Stirling cycle coolers have been used in cryogenic applications since 1940s. The first Stirling coolers for space application were developed in 1950s [5] and in the early 1960s the Stirling cycle appears to be an interesting challenge for domestic refrigeration [6-7]. The development has increased under the influence of growing environmental policies and Stirling refrigerating technology may be a rival to vapour compression systems.

Different authors established the optimal performances of irreversible Stirling refrigerator for given cooling load [8], by the way of finite time thermodynamics and comparison with test results [9-10]. Le'an [11] presented experimental results on a V-type integral Stirling refrigerator consisting of an expansion cylinder, a compression cylinder and a heat exchanger in-between. The parameters such as the power consumption and the coefficient of performance (COP) were investigated under various rotating speeds and charged pressures. More recently, Djetel et al. [12] and Getie et al. [13] compared the numerical and experimental performances of a Beta Stirling refrigerator. This article presents experimental characteristics of a Beta Stirling refrigerator at intermediate temperature range to achieve temperatures between -70°C and 20°C and heat lifts between 25 W and 650 W.

2. Description of the experimental setup

2.1. Prototype Stirling refrigerator

The Stirling refrigerator consist of a Beta-type architecture associated to a crank-rod mechanism that includes a working piston, a displacer piston, a compression volume, an expansion volume and a volume occupied by a regenerator (Figure 1). The working piston compresses and expands the fluid, while the displacer piston displaces the gas between the hot and cold parts of the machine, thus ensuring the isochoric transformations of the ideal Stirling cycle. The regenerator stores the heat of the fluid during the transfer of the gas from the hot part to the cold part and releases it in the opposite direction. Two heat exchangers are placed, one at the cold source and one at the water-cooled hot sink. The lower part of the machine contains the connecting rods and the crankshaft. The volume of the lower part is also pressurized and called the bounce space.

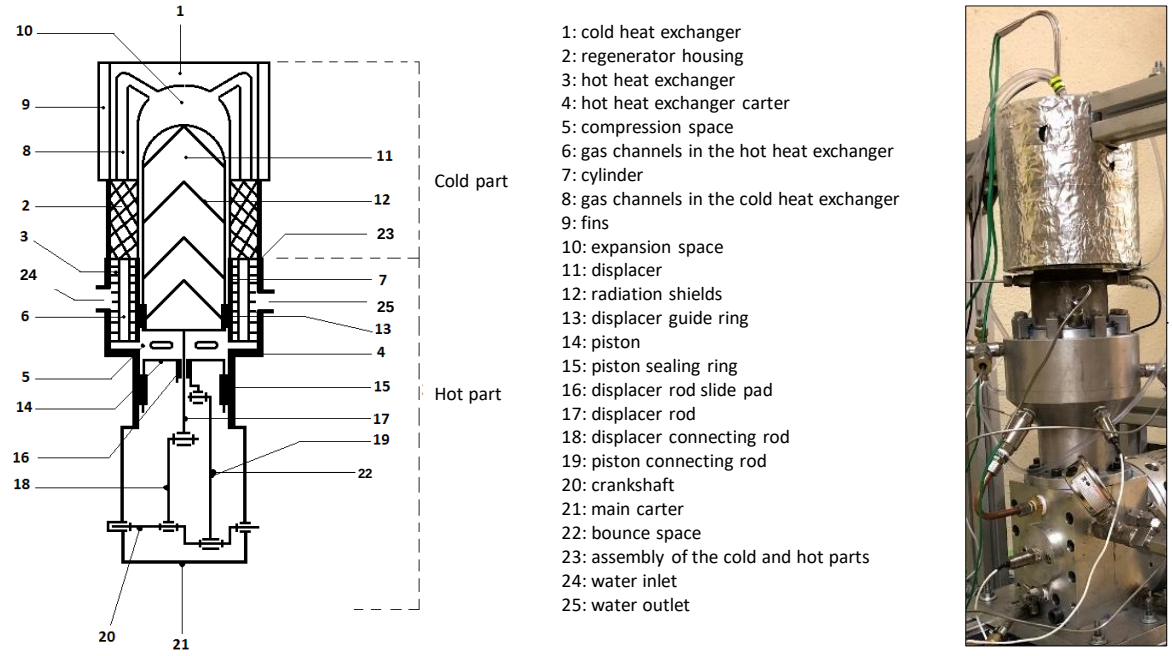

Figure 1. Schematic view and photo of the cold part of the machine

2.2. Technical specifications

The Stirling refrigerator is designed to operate with nitrogen at a mean pressure between 15 bar and 20 bar. The observed cooling capacity is 4750 W at 0 °C and 220 W at -37°C for the pressure 16 bar. The specifications of the machine are presented in Table 1. The material used is stainless steel for the cold head and aluminum for the radiator at the hot sink.

2.3. Test system

The driving module consists on a 11 kW asynchronous electric engine associated with a 11 kW inverter (Figure 3). The rotational speed is controlled in open loop by the inverter indicates its electric power. A torque and velocity sensor (Dataflex 32 - 300 N.m +/-0.5%) is inserted in the shaft. The top dead center of the displacer is detected by a magnetic sensor mounted on the shaft. The rotating motion of the motor shaft is converted through the crank-rod mechanism to reciprocating linear motions of the piston and the displacer with a fixed 90° phase difference. The compression volume is water-cooled and

the cooling water flowrate is measured by a variable area flowmeter (Brooks GT1024 22000 l.h-1 accuracy 2% of the full scale).

Table 1. Technical specifications of the refrigerator

Refrigerator characteristics	Specifications
Working gas	Nitrogen
Regenerator	Stainless steel wire mesh
Cooling capacity at 0°C	550 W
Cold end temperature	-80 °C < T_C < 20 °C
Hot sink temperature	T_H = 30°C
Mean Pressure	15 bar < P < 18 bar
Width x Height x Depth	0.19 m x 0.46 m x 0.18 m
Power piston diameter	$d = 6.10^{-2}$ m
Power piston stroke	$C = 4.10^{-2}$ m
Compression swept volume	$V_{swc} = 120.10^{-6}$ m^3
Rotational speed	35 rad.s^{-1} < ω < 80 rad.s^{-1}

An electric heated collar is used to apply a thermal load on the cold head. Its electric power is adjusted with a variable transformer and measured by a wattmeter. This value is considered as the heat lift L of the refrigerating machine. The pressures of the compression and expansion volumes are measured by two pressure transducers Kulite ETM-DC-375 35 bar and EWCTV-31-35 bar respectively. The pressure sensor at the cold end is heated by a water circulation at ambient temperature to prevent its damage due to the low temperature. Therefore, it applies an additional thermal load on the cold end and is removed when the expansion pressure measurement is not used. Figure 5 presents the parameters measured on the refrigerator. The temperatures are measured by K thermocouples (accuracy +/-1.5°C) at the outside of the cold head of the machine (T_{ext}), at the inlet and outlet of the cooling water ($T_{water,in}$ and $T_{water,out}$), in the expansion and compression space (T_e and T_{co}), and at the edges of the regenerator ($T_{reg,inf}$ and $T_{reg,sup}$). The data are acquired with a sampling period of 1 ms and then smoothed with a numerical filter.

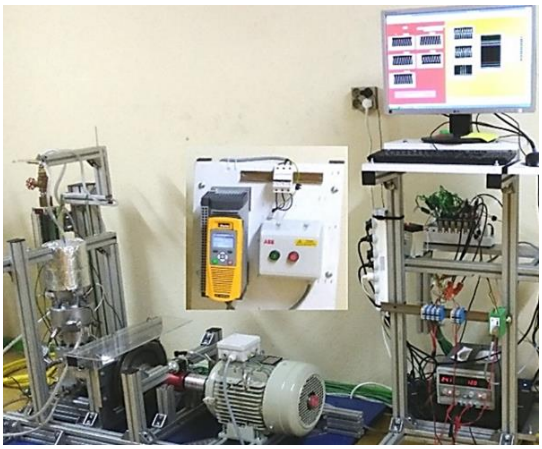

Figure 3. Refrigerator, power control and data acquisition system

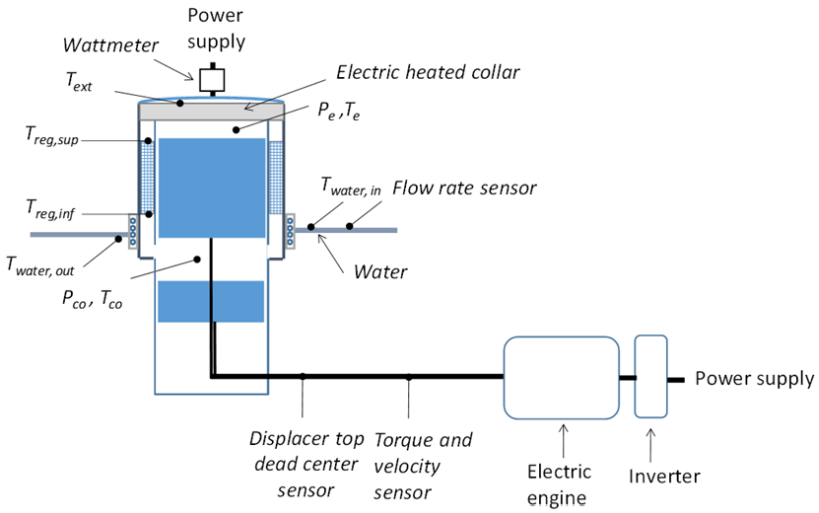

Figure 4. Schematic diagram of the measurement parameters

3. Experimental results and analyses

Experiments are presented for two cases : without thermal load and with thermal load.

3.1. Refrigerating characteristics without thermal load

This first set of experiments, referred as "no load" tests, give the performances of the machine without thermal load, i.e. no heating is applied on the cold end of the machine. These results are a working base used as a reference. The cold head of the Stirling refrigerator is insulated. Therefore, the heat load corresponds to the heat exchange with the environment by natural convection with ambient only due the imperfection of the insulation (with 3 mm thick and its conductivity is estimated at 0.05 $W.m.K^{-1}$). The calculated heat flux absorbed by the cold head surface is about 25 W.

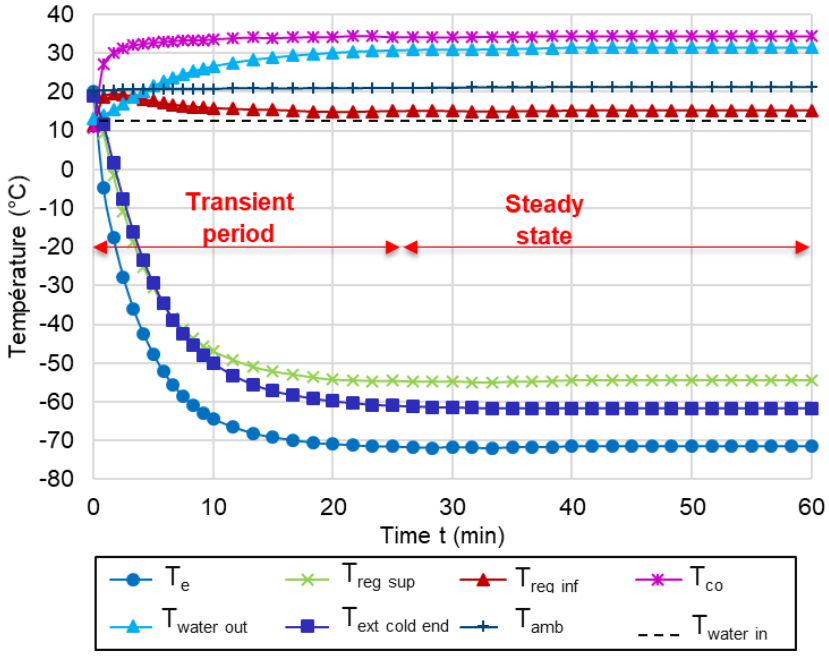

Figure 5. Evolution of the temperatures in the different volumes and on the external face of the cold head without a load as a function of time (Pressure 16 bar – Rotational speed 725 rpm)

The duration of the transient period is around 25 minutes after which the machine operates in steady state. We observe a temperature difference ($T_{reg\ inf} - T_{reg\ sup}$) of 70°C between the inlet and the outlet of the regenerator.

The Pressure-Volume diagrams of the expansion and compression spaces are plotted in Figure 6. As the Stirling engine is operated in reversed cycle, the area of the compression space PV diagram is larger than the expansion space area. The thermodynamic work W associated to the expansion and compression transformations is computed by numerical integration of $W = -\int PdV$. The computed thermodynamic work and power of the compression and expansion spaces are 99 J, 1172 W, and -58 J and -670 W respectively.

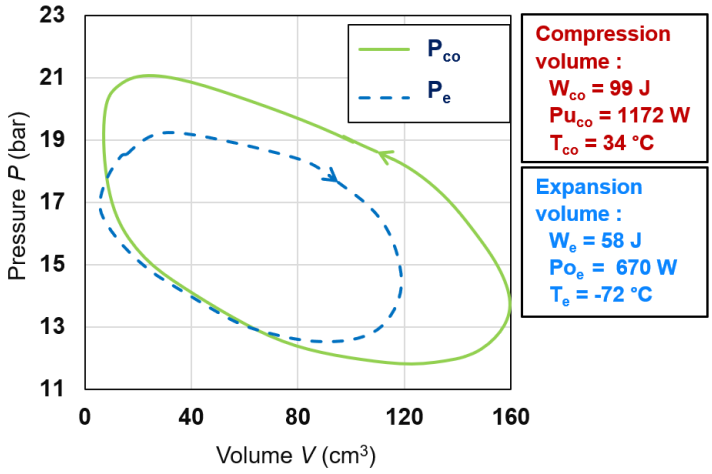

Figure 6. Pressure-Volume diagrams of the expansion and compression spaces without load (Pressure 16 bar – Rotational speed 725 rpm)

The temperature on the external face of the cold head (or that of the gas in the expansion volume) stabilizes after the transient phase, at a value that also depends on the speed of rotation. The results in Figure 7 show that for a speed N = 295 rpm, the stabilized temperature on the external face of the head is T_{ex} = -82°C while at N = 725 rpm, this stabilized temperature T_{ex} is equal to -76°C. For each speed, the difference between the temperatures in the expansion volume (gas) and on the external face of the head (wall) corresponds to the heat loss in the solid wall of the cold head. As the machine is not lubricated, it works best at low speed. At a lower speed, the achieved cold temperatures are higher due to a lack of power. At a higher speed, the temperatures also raise probably due to an increase in the losses. Figure 7 shows that there is a local minimum: the coldest temperature on the outer face or in the expansion volume of the head is obtained with a drive speed of 435 rpm, for a filling pressure of the Stirling machine at 16 bar. This type of result was also observed by Wu et al [14].

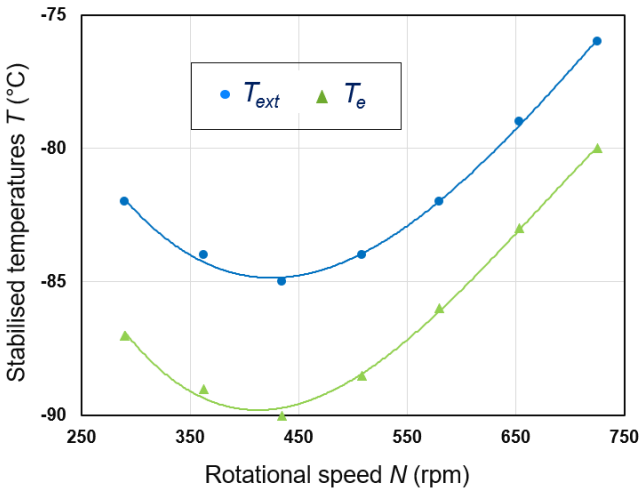

Figure 7. Stabilized temperatures in the expansion volume and on the external face of the head as a function of the machine speed (Pressure 16 bar).

3.2. Refrigerating characteristics with thermal load

The thermal load is imposed by a ceramic electric heating collar (1.2 kW maximum) for the characterization (Figure 4). The electric power of the heat load represents the heat lift of the machine The heating power of the collar is controlled by an alternator. In order to limit the heat loss between the heating collar and the cold head of the machine, the whole assembly is thermally insulated by a mattress specially designed for such applications. The power absorbed by the electric heating collar is measured by a wattmeter. As the Stirling machine is non-lubricated, its maximum driving speed by the three-phase asynchronous motor is set at 725 rpm in order to minimize dry friction and therefore mechanical losses.

The measurements obtained are shown in Figure 8. In this test, the electric heater power is set at 220 W. At the beginning of the test, we observe that all temperatures are around 20 °C. When the Stirling machine is switched on, the temperatures in the cold zone (in the expansion volumes and above the regenerator, and on the outside of the head) fall. The temperature in the expansion volume reaches -61 °C. After a short stabilization period, the electric heating collar is switched on with a heating power of 220 W, its faster dynamics than that of the Stirling machine causes the cold temperatures to rise. Operation is then continuous until all temperatures have stabilized: steady state is reached at a cooling capacity of 220 W with a temperature on the outside of the head of -37 °C.

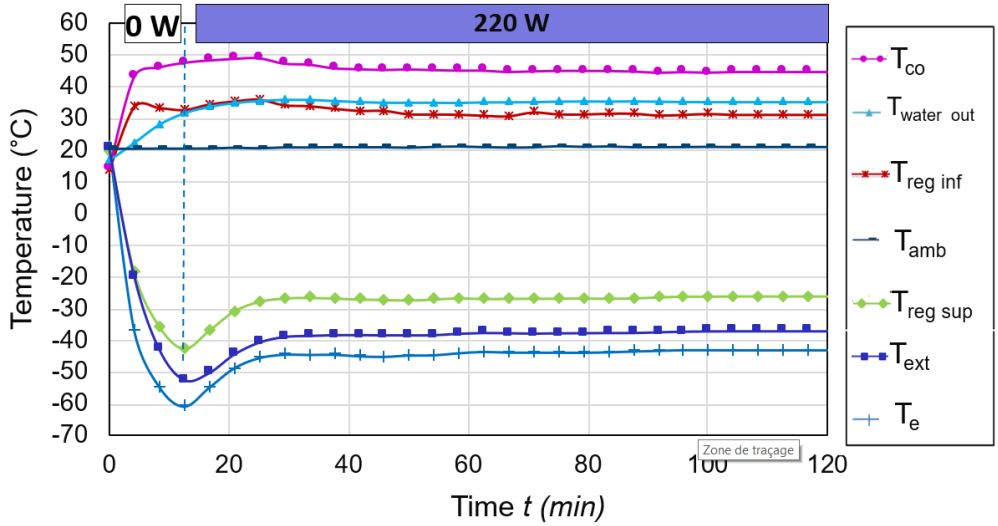

Figure 8. Evolution of the temperatures in the different volumes and on the external face of the cold head with a 220 W load as a function of time (Pressure 16 bar – Rotational speed 725 rpm)

The Pressure-Volume diagrams of the expansion and compression spaces are plotted in Figure 9. The computed thermodynamic work and power of the compression and expansion spaces are 93 J, 1120 W, and -52 J and -630 W respectively. When the refrigerator reaches its stabilisation regime (after 30 minutes), the temperatures of the compression and expansion volumes are T_{co} = 45°C and T_e = -43°C respectively.

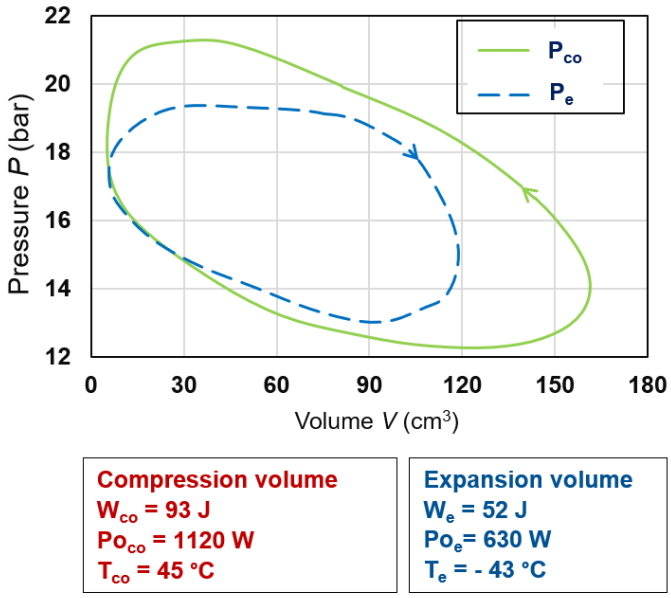

Figure 9. Pressure-Volume diagrams of the expansion and compression spaces with a 220 W load (Pressure 16 bar – Rotational speed 725 rpm).

Figure 10 shows the changes in temperature T_{ext} on the external face of the machine head as a function of the cold power produced and time. After a transitional phase, an equilibrium temperature is achieved for each thermal load. For zero power, i.e. no thermal load, the temperature stabilised at -61°C after 30 min. For negative cold production, temperatures range from -37°C to 0°C and power ratings vary from 220 to 475 W. For positive cold productions, temperatures range from 0 °C to 20 °C and power ratings vary from 475 to 653 W.

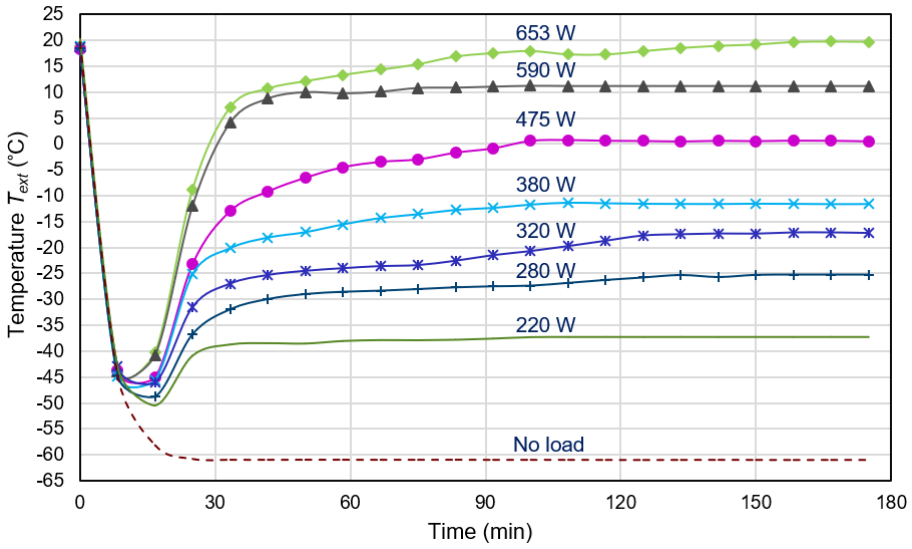

Figure 10. Temperature evolutions as a function of time on the external face of the head with different cold productions from 0 (no load) to 653 W (pressure 16 bar – rotational speed 725 rpm).

The Carnot coefficient of performance (COP_{Carnot}) is defined as the heat Q_e removed from the cold reservoir divided by the work W done to remove the heat. For an ideal refrigerator, without losses and irreversibilities (first law of thermodynamics):

$$COP_{Carnot} = \frac{Q_e}{W} = \frac{Q_e}{Q_c - Q_e} = \frac{T_e}{T_c - T_e} \tag{1}$$

The real coefficient of performance COP_{real} is the ratio of the lift L (power load at the cold reservoir) and the absorbed electric power $\dot{W}_{elect}$ by the electric motor.

$$COP_{real} = \frac{L}{\dot{W}_{elect}} \tag{2}$$

Consequently, we define the refrigerator efficiency E (%) as the ratio of the real and Carnot coefficients of performance:

$$E(\%) = 100\frac{COP_{real}}{COP_{Carnot}} \tag{3}$$

The evolutions of the different coefficients of performance are described in Figure 11. At the observed low temperature of -37 °C, the cold production (Lift) is 220 W with an actual real experimental COP of 0.12 and a Carnot COP of 2.88. At the temperature of 20 °C, the cooling output is 652 W with an actual COP of 0.45 and a Carnot COP of 10.50. It can be seen logically that the COP increase with the temperature measured on the external face of the head.

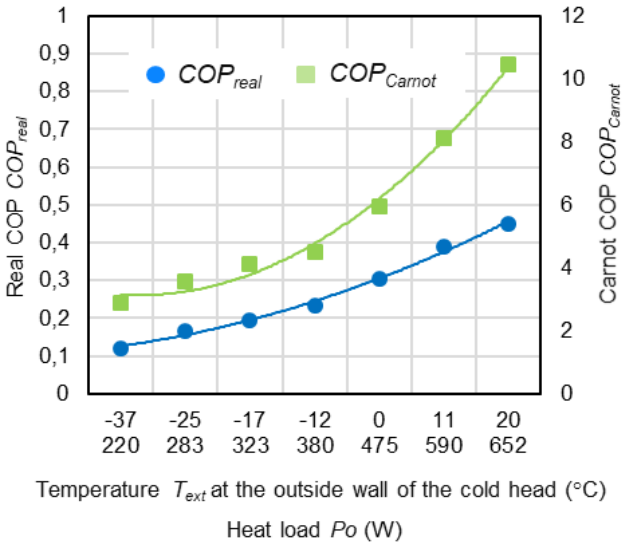

Figure 11. Carnot and real coefficients of performance function of the temperature at the outside wall of the cold head and the heat load (Lift).

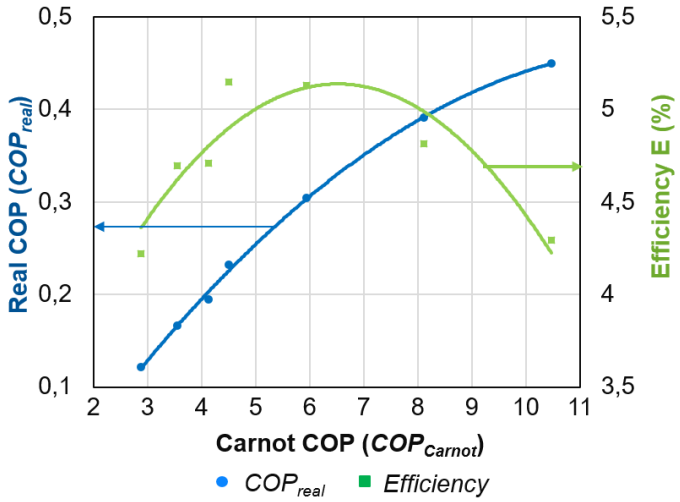

Figure 12. Real COP and efficiency of the refrigerator function of the Carnot COP

4. Conclusion

We have carried out experimental results of a Beta Stirling machine operating with nitrogen as a refrigerating machine operating at intermediate temperature range. The aim is to study alternative technologies to vapour compression machines and works presented in this paper support the following conclusions. For zero power, the evolution of the performance of the machine with the rotational speed was studied. The refrigerator performance shows an optimal speed to produce the coldest temperature on the outer face (-85°C) and in the expansion volume (-90°C) of the head with a drive speed of 435 rpm.

For zero power, i.e. no thermal load, the temperature stabilised at -61°C at 725 rpm. For negative cold production, temperatures range from -37°C to 0°C and power ratings vary from 220 W to 475 W. For positive cold productions, temperatures range from 0 °C to 20 °C and power ratings vary from 475 to

653 W. The experimental coefficient of performance was determined and compared to the Carnot coefficient of performance. At the temperature of -37 °C, the cold production (Lift) is 220 W with an actual COP of 0.12 and a Carnot COP of 2.88. The influence of the charge pressure was also analyzed.

Acknowledgments
This work has been supported by EIPHI Graduate School (contract ANR- 17- EURE- 0002) and the Region Bourgogne-Franche-Comte, by Bahir Dar Institute of Technology, by the Embassy of France to Ethiopia and the African Union, and by the Ministry of Science and Higher Education of Ethiopia.

References

[1] Sun J, Im P, Bae Y et al. 2021 *Sci Data*, 8, **144** 1
[2] Mota-Babiloni A, Navarro-Esbrí J, Barragán-Cervera A, Molés F, Peris B, Verdú G 2015, Int. J. of Refrigeration, **57**, 186
[3] IIF-IIR 2019, *The role of refrigeration in the global economy*, 38th Informatory Note on Refrigeration Technologies, June
[4] Walker G and Reid Bingham E 1994 *Low-capacity cryogenic refrigeration*. **9** (Oxford University Press, Oxford)
[5] Finkelstein T and Polonski C 1959, *Development and testing of a stirling cycle machine with characteristics suitable for domestic refrigerators*. Report W/M (3A).u.5, (English Electric Company Ltd., Whetstone)
[6] Walker G 1987 *Cryocoolers*, (Plenum Press)
[7] Urieli I and Berchowitz D M 1984, *Stirling Cycle Engine Analysis*. (Adam Hilger Ltd, Bristol)
[8] Chen J 1998 *Energy Conv. Management.* **39** 1255
[9] Chen L, Wu C and Sun F 1998 *Energy Conv. Management.* **39** 117
[10] Lundqvist P, 1991 *Proc. of 18th Int. Cong. Of Refrigeration*. Montreal, Paper 65
[11] Le'an, S., Yuanyang, Z., Liansheng, L. and Pengcheng, S 2009 *App. Therm. Eng.* **29** 210
[12] Djetel-Gothe S, Bégot S, Lanzetta F and Gavignet E 2002 *Int. J. of Refrigeration*, **115**, 96
[13] Getie M Z, Lanzetta F, Bégot S., Admassu B.T. 2021 Entropy: Thermodynamics – Energy – Environment – Economy, **2**, 1
[14] Wu X.L., Chen L.B., Pan C.Z., Cui C., Wang J.J. and Zhou Y. 2017 *Conf. Ser. Mater. Sci. Eng.,* **278**, 12151